Responses to reviewer comments

In this response letter, we provide a point-by-point response to each comment. The original comments are in *blue italic font*, and our responses are in black font. Changes made in the manuscript are highlighted in the text with line numbers referring to the **tracked-changes PDF version** (manuscripts_v6_track_change.pdf).

Reviewer #1:

Review of manuscript titled: "Transport Efficiency of Turbulent Parcel in the Marine Boundary Layer and Its Implications for Droplet Activation in Marine Cloud Brightening"

Authors: P. Zhao, J. Chen, Y. Yang, Y. Jia, and Y. Yu

General comments:

In this study, nested WRF simulations of a few stratocumulus days over the southeast Atlantic are coupled with FLEXPART-WRF to assess the efficiency of aerosol delivery in the context of MCB. Overall, the authors find that, for the limited environments examined, the aerosols are rapidly transported to the cloud layer and activation fractions exceed 70%. I find the overarching framework to be attractive, particularly the combination of WRF, FLEXPART-WRF, and simple representations of activation. However, I have several major questions surrounding each stage of the analysis.

1.) Nested LES: It is unclear that the LES domain (WRF d04) is performing better in comparison to the lower-resolution nested domains. In fact, it looks like the LES is performing more poorly than the coarse grid for LWP (Fig. 2). If running WRF at LES grid spacing actually degrades model performance, does it provide any additional benefit to the study? I think there needs to be some effort to improve the performance of the LES with respect to the observations, which may require boundary layer profile sharpening and/or initial condition corrections (Erfani et al., 2025) and comparisons to variables other than strictly LWP (compare to SW cloud radiative effect from CERES, for example).

Thank you for this comment. We have revised the manuscript to address the comments raised by the reviewer, as detailed below.

(1) Clarification of the evaluation framework and the role of d04.

The discrepancy between d04 and the available LWP observations does not by itself indicate poorer model performance, because the available observations and the nested WRF domains differ substantially in spatial scale and sampling, and the available observations are insufficient to directly determine which resolution provides a more accurate representation of the cloud field. Nevertheless, the comparison with observations shows that the simulations in general capture the observed cloud evolution during the study period. Therefore, d01 is primarily evaluated by observation, while d02-d04 are used to investigate resolution-dependent turbulent transport and cloud-base processes.

(2) Boundary-layer profile sharpening and initial-condition corrections.

Boundary layer profile sharpening and initial-condition corrections would be promising ways to improve the simulations. However, we did not apply them in this study for three reasons. First, we lack high-resolution observations to verify whether the revised simulations are actually improved. Second,

we selected the case in which the low cloud fraction most closely matches satellite observations (Fig. R1), ensuring that the boundary layer forcings from the ERA5 reanalysis are among the most accurate available for this case. Third, these approaches do not directly modify the d04 simulation, because the inner d04 domain is driven by the outer-domain solution as boundary forcing.

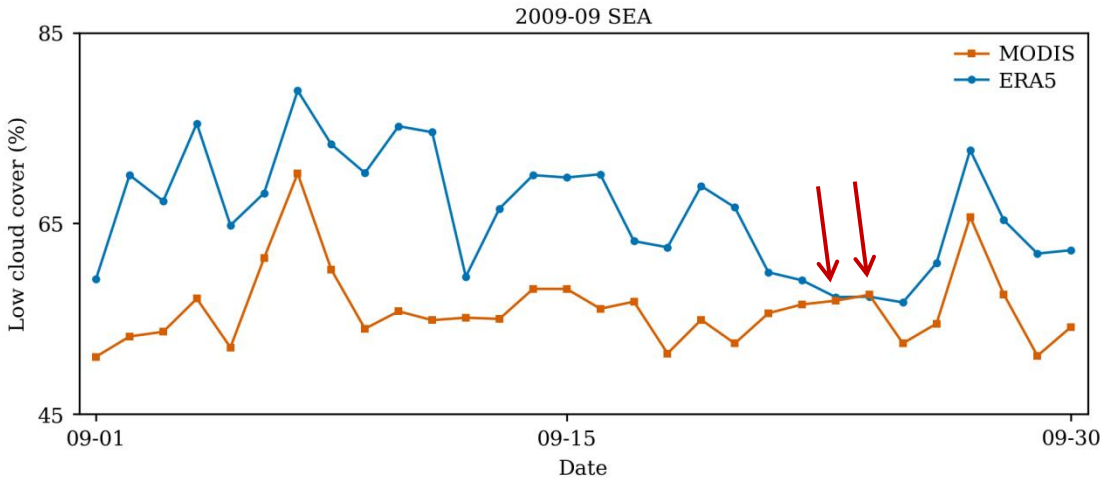


Figure R1. Daily low cloud cover (%) over the SEA during September 2009 from ERA5 reanalysis (blue circles) and MODIS satellite observations (vermillion squares).

(3) Additional observational evaluation.

As suggested by the reviewer, we have added comparisons of SWCRE and CBH with CERES and CALIPSO observations, respectively, in addition to LWP. These comparisons are presented in Fig. 2 and discussed in Sect. 3.1.

Modifications in the main text that are relevant to this comment:

Sect. 2.1 (Lines 101-107): We have added a description of the used ERA5 variables when we select the case and evaluate the model simulations with observations: “In addition, several ERA5 variables are used during case screening and the evaluation of the simulated cloud evolution: CBH, total column liquid water (tclw; i.e., the scene-averaged LWP), and net solar radiation under all-sky and clear-sky conditions at both the top of the atmosphere (tsr, tsrc) and the surface (ssr, ssrc). The hourly accumulated radiation fields (tsr, tsrc, ssr, ssrc) in ERA5 are converted to hourly-mean fluxes, while the high-frequency WRF outputs (15 min for d01 and 1 min for d04) are likewise averaged to 1-hour intervals, enabling temporally aligned evaluations of TOA and surface SWCRE against both ERA5 and CERES satellite observations.”.

Sect. 2.2 (Lines 115-136): We have added descriptions of the CERES and CALIPSO data and their processing: “To evaluate the simulated SWCRE, we use the CERES SYN1deg-1H Edition 4.2 (Edition4B) product (Rutan et al., 2015), covering 23 – 25 September 2009. This product combines CERES instrument observations from the Terra and Aqua satellites with temporally interpolated geostationary satellite data, providing TOA and surface radiative fluxes at a horizontal resolution of

$1^{\circ} \times 1^{\circ}$ and a temporal resolution of 1 h. In this study, SWCRE is uniformly defined as the difference between all-sky and clear-sky net shortwave fluxes (negative values indicate a cloud cooling effect); for CERES, it is derived from the difference between all-sky and clear-sky downward and upward shortwave fluxes at both the TOA and the surface, while the corresponding variables and conversions for WRF and ERA5 are described in Sects. 2.4 and 2.1, respectively.

To evaluate the simulated CBH, we use the 5-km merged layer product (CAL_LID_L2_05kmMLay, Version 5–00) from the CALIOP aboard the CALIPSO satellite, covering 23 September 2009. The product reports the boundaries of cloud and aerosol layers along the orbit; here we use its single-shot profiles, which have an along-track horizontal resolution of approximately 333 m. Within the study region (14.65°S – 10.00°S, 10.00°W – 5.70°W), CALIPSO passed over the region twice on 23 September, at 01:47:38 UTC and 14:06:05 UTC; no overpass covers the region on 24 September, so the CBH comparison is restricted to 23 September. The CBH is extracted profile by profile. For each single-shot profile, the reported layers are examined from the lowest one upward; layers classified as non-cloud (clear air or aerosol) and layers with a cloud − aerosol discrimination (CAD) score below 70 are discarded, and the first remaining cloud layer is taken as the lowest cloud layer of that profile. The CBH above ground level (AGL) is then obtained by subtracting the surface elevation from the layer-base altitude, which is referenced to mean sea level. Consistent with the model and reanalysis, only low-cloud samples with an AGL cloud base below 3 km are retained: a profile is excluded if its lowest cloud base exceeds 3 km or if it contains no qualifying cloud layer. The comparison with the model is constructed under two spatial configurations: over the d01 region, the profile cloud bases are averaged onto the 0.25° grid, whereas over the d04 region, the original single-shot footprints are retained; the detailed spatial and temporal collocation is described in Sect. 3 and in the caption of Fig. 2.".

Sect. 2.4: We have added descriptions of SWCRE and CBH in the WRF simulations, including "the downward and upward shortwave fluxes at TOA (SWDNT and SWUPT) together with their clear-sky counterparts (SWDNTC and SWUPTC), and the corresponding surface fluxes (SWDNB, SWUPB, SWDNBC, and SWUPBC)" (Lines 172-174), as well as "SWCRE at both the TOA and the surface is derived from these fluxes and their clear-sky counterparts. The WRF CBH is defined as the height above ground of the lowest model level with QCLOUD $\geq 10^{-6}$ kg kg^{-1}, and, consistent with CALIPSO (Sect. 2.2) and ERA5 (Sect. 2.1), only columns with a cloud base below 3 km are retained; the identical diagnostic is applied to d01 and d04 (Fig. 2d)." (Lines 176-179)

The corresponding evaluation results are presented in the revised Sect. 3.1 (Lines 258-289): "To evaluate the simulated cloud field and boundary-layer structure, Fig. 2 compares WRF LWP, SWCRE, and CBH with MODIS, CERES, CALIPSO, and ERA5. WRF d01 reproduces the observed increase in LWP from 23 to 24 September indicated by MODIS, whereas ERA5 shows the opposite trend (Figs. 2a, b). Although d04 captures the same trend as MODIS, its mean LWP is 43 – 44 % lower than that of WRF d01 sampled over the d04 region, highlighting substantial resolution sensitivity. However, the fine resolution and limited spatial coverage of the d04 domain limit direct comparisons with coarse-resolution satellite observations; model evaluation therefore focuses primarily on d01. The higher-resolution domains are primarily used to diagnose resolution-dependent turbulent parcel transport and cloud-base activation, rather than to demonstrate improved agreement with

regional-mean observations. Both WRF and ERA5 slightly underestimate the magnitude of SWCRE (Fig. 2c). Both WRF and ERA5 also underestimate CBH relative to CALIPSO (Fig. 2d), with similar bias magnitudes for WRF d01 and ERA5. Overall, WRF captures the observed cloud evolution while exhibiting resolution-dependent differences in cloud properties, providing a basis for investigating turbulent transport across grid spacings.

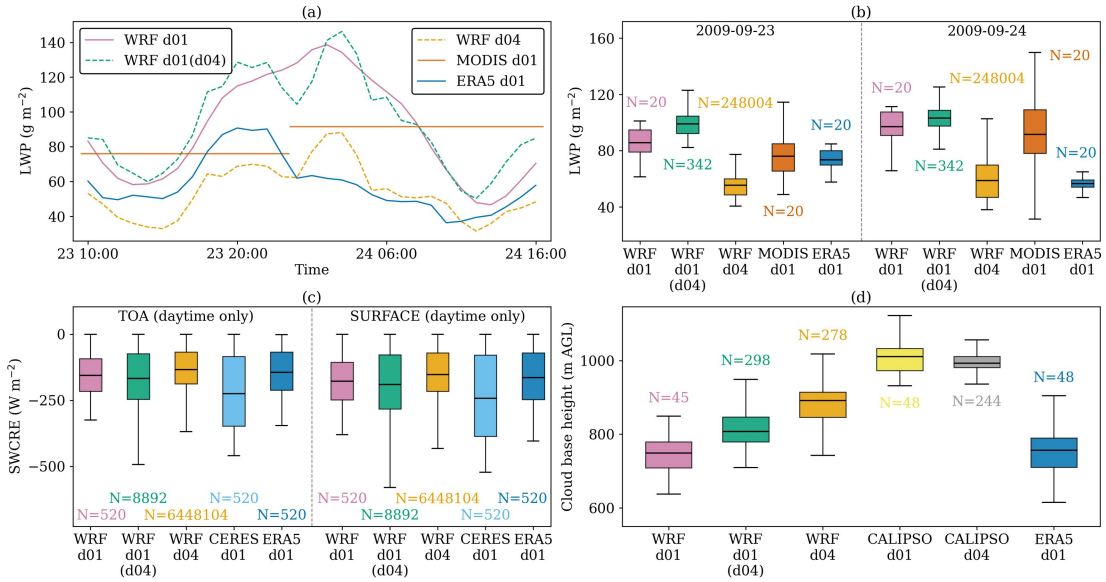


Figure 2. Comparison of cloud and boundary-layer characteristics between WRF simulations, ERA5 reanalysis, and satellite observations. (a) Temporal evolution of LWP from 10:00 UTC on 23 September to 16:00 UTC on 24 September 2009. WRF d01, WRF d01(d04) (i.e., WRF d01 clipped to the d04 region), and WRF d04 are 1-hour averages, ERA5 provides hourly data, and MODIS provides daily means. (b) Boxplots of daily-mean LWP for 23 – 24 September. WRF d01 and ERA5 are matched to a 1° grid, WRF d01(d04) and WRF d04 retain their native grids, and MODIS is provided on its native 1° daily grid. (c) Boxplots of 1-hour mean TOA and surface SWCRE during daytime on 23 – 24 September, with data over the d01 region uniformly matched to a 1° grid, while WRF d01(d04) and WRF d04 retain their native grids. (d) Boxplots of CBH during two CALIPSO overpasses (01:47:38 and 14:06:05 UTC) on 23 September 2009; no CALIPSO data are available over the entire d01 region on 24 September. For the d01 region, CALIPSO, WRF, and ERA5 data are matched to a 0.25° grid, whereas for the d04 region, WRF d01 and WRF d04 are interpolated along the CALIPSO track to the original footprint locations. For both regions, ERA5 and WRF data are temporally matched to the CALIPSO overpass times with the corresponding spatial matching procedures. In the boxplots, boxes represent the interquartile range (IQR), and black horizontal lines indicate means; the corresponding statistics and sample size N are labeled adjacent to each box. In panel (a), WRF d01 (solid line), WRF d01(d04) (dashed line), WRF d04 (dashed line), MODIS d01 (solid line), and ERA5 d01 (solid line) are compared. Colors are kept consistent throughout the figure: WRF d01, WRF d01(d04), WRF d04, MODIS d01, ERA5 d01, CERES d01, CALIPSO d01, and CALIPSO d04 are shown in reddish purple, bluish green, orange, vermillion, blue, sky blue, yellow, and grey, respectively. All d01 data are extracted from the clipped region (14.65°S – 10.00°S, 10.00°W – 5.70°W; Fig. 1a).”

(4) Scientific value of the higher-resolution domains.

The main value of d04 is that it takes advantage of the additional dynamical and process-level information provided by the finer spatial resolution to address the scientific questions, rather than comparing with regional-scale observations. Specifically, the higher resolution provides more detailed cloud-field structures (as illustrated in Fig. 1) and vertical-motion information, allowing us to better diagnose turbulent parcel transport, cloud-base updrafts, and the associated aerosol activation processes. As stated in Sect. 3.1, “These finer-scale structures provide more detailed representations of cloud and boundary-layer variability for subsequent parcel transport analysis.” (Lines 246-248).

We have clarified in Sect. 3.1 that "However, the fine resolution and limited spatial coverage of the d04 domain limit direct comparisons with coarse-resolution satellite observations; model evaluation therefore focuses primarily on d01. The higher-resolution domains are primarily used to diagnose resolution-dependent turbulent parcel transport and cloud-base activation, rather than to demonstrate improved agreement with regional-mean observations." (Lines 262-265).

Our study explores the sensitivity of transport efficiencies to model grid spacing. This purpose is specified in Sect. 2.4: "the nested d02 – d04 design is therefore used to quantify the sensitivity of the diagnosed parcel transport and cloud-base activation to grid spacing (Sects. 3.3–3.4)" (lines 159-160).

2.) FLEXPART-WRF: I'm confused by the connection between the nested LES and the particle modeling. My initial expectation was that the LES turbulence properties (variances and dissipations rates) would be used to directly drive the particle model, as was done for horizontal transport in McMichael et al. (2024, 2026). If I'm interpreting the current setup correctly, the author's use TURB_OPTION = 1 in FLEXPART-WRF, which uses a Hanna-type boundary layer turbulence scheme to estimate the turbulence properties. This seems like an unnecessary step when you have direct access to the relevant turbulent parameters.
More importantly, we do not necessarily expect a subgrid TKE or boundary layer closure to improve monotonically as grid spacing decreases. As the grid spacing is reduced from 2.7 km to 100 m, the partitioning between resolved and subgrid turbulence changes, and the assumptions underlying eddy diffusivity or Hanna-type boundary layer closures may become inapplicable to LES scales. Can the authors clarify what turbulence/boundary layer quantities from WRF are actually used by FLEXPART-WRF in this configuration, and why TURB_OPTION = 1 is appropriate for the 100 m domain?
I also encourage the authors to consider additional calibration tests. For example, why not inject passive tracers directly into the WRF domain at several release locations and compare their dispersion with FLEXPART-WRF? Ideally, a sea salt aerosol plume could be simulated directly in WRF-CHEM. Demonstrating that the WRF-FLEXPART method reproduces the plume evolution from a WRF-CHEM or passive tracer simulation would provide a compelling validation step and would make the FLEXPART-WRF framework more useful for future MCB transport studies.
Thank you for this comment. Our clarifications and modifications to the manuscript are described below.

(1) Coupling method of FLEXPART-WRF and WRF
The coupling method is described in the revised manuscript (Sect. 2.5, Lines 182-190): "We use FLEXPART-WRF (i.e., FLEXPART configured to use WRF output as input, version 3.2; Brioude et al., 2013) to simulate Lagrangian transport of turbulent parcels within the marine boundary layer, driven by three-dimensional WRF meteorological fields (Table 1). The fields passed from WRF to FLEXPART include winds, pressure, geopotential, temperature, water vapor, and near-surface meteorological variables. Turbulent dispersion is represented using the Hanna et al. (1982) parameterization, which diagnoses turbulent velocity fluctuations and Lagrangian time scales rather than directly using WRF turbulent kinetic energy (TKE). Although this scheme may not be optimal at LES resolutions (Cornwell et al., 2021), it is applied consistently across domains to provide a common

baseline for assessing differences in transport efficiency associated with the resolved air motion. Boundary-layer height is diagnosed internally using a critical Richardson number method (Vogelezang and Holtslag, 1996)."

(2) Why TURB_OPTION = 1 is retained

We agree that a parameterized turbulence treatment should not be assumed to become more appropriate simply as the WRF grid spacing approaches LES scales. Our original choice of TURB_OPTION = 1 followed the recommendation of Brioude et al. (2013), whose evaluations on the available turbulent-dispersion options identified violations of the well-mixed criterion in the WRF-TKE-based options. This provides a rationale for selecting the recommended Hanna scheme, but does not demonstrate its validity for the 100 m domain.

Using WRF turbulence directly also requires a consistent treatment of the velocity variances, Lagrangian time scales, and turbulent drift. Because the LES wind fields already represent part of the turbulent motion, the additional stochastic velocities should only represent the part of turbulence unresolved by the input fields. Switching to WRF-TKE option alone does not guarantee the consistency.

We acknowledge that the Hanna scheme used here does not explicitly adjust its prescribed turbulence to account for the fraction resolved by LES, and as pointed out by Cornwell et al. (2021), this may cause overlap between resolved and parameterized turbulent motions. In our configuration, we retain TURB_OPTION = 1 as a common baseline across d02-d04 for the resolution-sensitivity experiments, rather than assuming that it becomes more physically appropriate at finer resolution. Using different turbulent options for different input resolutions would not help determine whether the differences arise from the different grid spacings of WRF as the input to FLEXPART or from the turbulence scheme in FLEXPART.

(3) WRF quantities used by FLEXPART-WRF.

We have clarified the WRF meteorological fields used as input to FLEXPART-WRF in Sect. 2.5 (Lines 182-185): "We use FLEXPART-WRF (i.e., FLEXPART configured to use WRF output as input, version 3.2; Brioude et al., 2013) to simulate Lagrangian transport of turbulent parcels within the marine boundary layer, driven by three-dimensional WRF meteorological fields (Table 1). The fields passed from WRF to FLEXPART include winds, pressure, geopotential, temperature, water vapor, and near-surface meteorological variables."

We have further clarified how our methodology differs from that of McMichael et al. (2024, 2026) (Sect. 2.5, Lines 192-195): "Our method is different from McMichael et al. (2024, 2026), who used an independent Langevin particle model driven by LES-derived turbulence statistics, such as velocity variances and turbulent dissipation rates, to investigate horizontal dispersion." This framework allows us to investigate vertical transport from near the sea surface to cloud base, as well as first-arrival times, cumulative transport efficiency, and in-cloud residence times. Because FLEXPART-WRF is used as an offline post-processing transport model, a single WRF meteorological simulation can be used to test different release locations, release times, release durations, and particle ensembles without rerunning the simulation. This flexibility is particularly useful for exploring alternative MCB release scenarios

under the same meteorological background. These considerations motivate our choice of a three-dimensional offline Lagrangian framework for investigating surface-to-cloud transport and its associated timescales.

(4) Additional calibration tests and WRF-Chem comparisons.
We agree that passive-tracer simulations in WRF, as well as WRF-Chem simulations with explicit aerosol processes, would provide useful comparisons for plume-scale transport. However, FLEXPART-WRF, as a mature post-processing Lagrangian trajectory tool (Brioude et al., 2013; Kazemirad and Miller, 2020; Cloux et al., 2021; Cornwell et al., 2021; Crespo-Otero et al., 2025; Chen et al., 2026), employs a different configuration, which makes direct comparisons with WRF-Chem plume simulations difficult. Our FLEXPART trajectories represent only air-parcel motion. Although aerosols or tracers may be assumed to follow these trajectories, their motion may also differ from air-parcel motion due to particle inertia and other aerosol-specific processes. Aerosol plume dispersion is influenced by both air-parcel motion and aerosol-specific processes. Our study focuses solely on background air-parcel transport, without explicitly representing aerosol-specific processes. Comparisons with passive-tracer simulations in WRF and explicit aerosol/plume simulations using WRF-Chem would be valuable but are beyond the scope of this manuscript and could be pursued in future work, as discussed in Sect. 4. The revised text is provided below:

"Because FLEXPART-WRF tracks passive turbulent parcels without explicitly representing aerosol-specific processes, the diagnosed transport efficiency reflects air-parcel transport rather than actual aerosol delivery. Future comparisons with passive-tracer simulations in WRF and with explicit aerosol/plume simulations using WRF-Chem could help distinguish uncertainties in turbulent transport from aerosol-specific effects." (Lines 624-628)

3.) Activation parameterization: The authors outlined a 2-D parameter space of number concentration and mean diameters, but FLEXPART-WRF should be able to explicitly provide 3-D concentrations from particle positions. Is there a reason the concentrations from FLEXPART are not used in the calculation of the activation? Since activation is inherently local and depends on the aerosol concentration reaching the cloud layer, this seems like a central quantity that should be linked directly to the particle simulation.
Thank you very much for this valuable comment. In this study, we use the air-parcel option in FLEXPART-WRF rather than the aerosol-particle option. Therefore, FLEXPART-WRF does not directly output aerosol number concentrations, but provides the spatial locations and trajectories of the released air parcels. For each WRF simulation, we release 50 000 air parcels. We diagnose the activation condition along each parcel trajectory and calculate the AF from the ensemble of parcels reaching the cloud base. Thus, we track air parcels rather than aerosol particles in this study.

We choose to track air parcels, because the differences between aerosol number concentrations at the sea surface and cloud base can also be affected by aerosol chemical processes and aerosol particles may not follow the same trajectories as air parcels because of their finite inertia. In addition, activation depends not only on aerosol number concentration but also on aerosol chemical properties and their effects on hygroscopic growth. A more detailed treatment using a cloud-parcel model will be considered in future work, as discussed in Sect. 4 (Lines 628-630): "while multimodal aerosol

representations and cloud parcel model simulations that resolve supersaturation and droplet growth over the in-cloud residence time could better constrain the full MCB transport − activation pathway".

Overall, I think the methodology has promise, especially using 2.7 km WRF simulations to drive FLEXPART-WRF, where Hanna-type closures are more appropriate. However, without some calibration or justification of FLEXPART-WRF at LES scales using TURB-OPTION = 1, I think the study should focus on the grid spacings that FLEXPART-WRF was originally designed for. Even at 2.7 km grid spacing, it would be nice to see a calibration study using injected MCB plumes. If it can be demonstrated that FLEXPART-WRF does a good job of recreating injected plumes in WRF (likely using both precipitating and non-precipitating cases, as the background environment can have a strong influence on the plume spreading dynamics (Prabhakaran et al., 2024; McMichael et al., 2024)), it opens the door to a WRF-ensemble study where this same type of analysis is done for a wide range of environmental conditions.

Thank you very much for the positive assessment of our 2.7 km WRF configuration and for the constructive suggestions regarding FLEXPART-WRF calibration, MCB plume injection, and ensemble simulations. We choose to use the same turbulent options across 2.7km-100m simulations, because using different turbulent options for different input resolutions would not help determine whether the differences arise from the different grid spacings of WRF as the input to FLEXPART or from the turbulence scheme in FLEXPART.

We would first like to clarify that the FLEXPART-WRF framework used here differs from explicit MCB plume-injection simulations. FLEXPART-WRF is driven by precomputed WRF meteorological fields and tracks passive air parcels without feedback to the background meteorology. Our objective is therefore to diagnose air-parcel transport efficiency and residence time from the near-surface marine boundary layer to the cloud layer under a prescribed meteorological environment, rather than to simulate the spatial evolution of an injected aerosol plume. This distinction is relevant to the studies suggested by the reviewer, Prabhakaran et al. (2024) and McMichael et al. (2024), which demonstrate that background environmental conditions, including precipitating versus non-precipitating conditions, can strongly affect plume dispersion. Explicit plume-injection simulations are therefore better suited for evaluating plume evolution and its two-way interactions with the background environment, whereas the present study focuses on the underlying air-parcel transport.

One advantage of our method is that FLEXPART, as a post-processing tool, can analyze response of trajectories to release timing, duration, location, and other parameters, without running expensive high-resolution simulations many times. This is another key strength of this study.

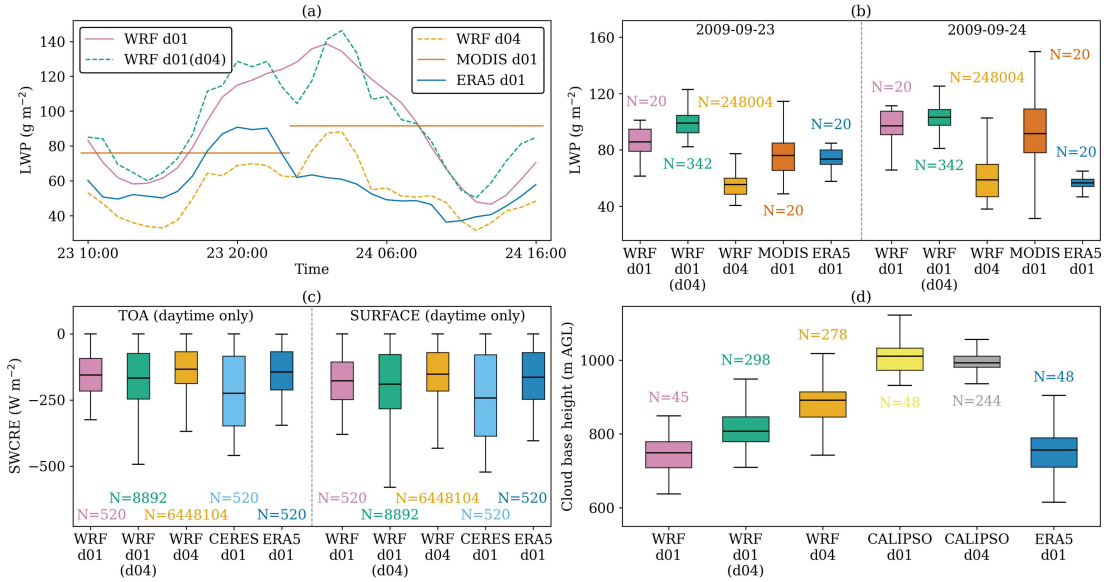
We agree that our analysis is limited to a single non-precipitating stratocumulus case and does not establish the applicability of the diagnosed transport characteristics to explicit MCB plume simulations. Comparisons with WRF passive-tracer simulations and explicitly injected aerosol plumes using WRF-Chem, together with analyses covering a wider range of regions, seasons, and meteorological conditions, would be valuable directions for future work. Such studies could also provide a basis for future WRF-ensemble investigations across a broader range of environmental conditions. Accordingly, we have revised Sect. 4 to clarify that FLEXPART-WRF diagnoses turbulent air-parcel transport rather than actual aerosol delivery, and to highlight these comparisons and broader environmental analyses as

priorities for future research. The revised text is provided below (Lines 623-630): “The analysis is limited to a single non-precipitating case, motivating future studies across broader regions, seasons, and meteorological conditions. Because FLEXPART-WRF tracks passive turbulent parcels without explicitly representing aerosol-specific processes, the diagnosed transport efficiency reflects air-parcel transport rather than actual aerosol delivery. Future comparisons with passive-tracer simulations in WRF and with explicit aerosol/plume simulations using WRF-Chem could help distinguish uncertainties in turbulent transport from aerosol-specific effects. Larger or periodic domains could reduce lateral parcel loss and sampling limitations, while multimodal aerosol representations and cloud parcel model simulations that resolve supersaturation and droplet growth over the in-cloud residence time could better constrain the full MCB transport–activation pathway.”.

Minor comments:

Figure 2: I would redoing this plot with lines that are easier to differentiate. Perhaps, only showing d01, d04 could reduce clutter?

We have redone the plots as below:



Lines 222-224: I think it’s important to mention that d04 (the LES domain) does not improve LWP agreement. Also, is this cloudy LWP in both WRF and MODIS, or scene-averaged LWP? You could get agreement in scene-averaged LWP while getting mesoscale morphology/cloud fraction completely wrong. This is why it’s important to compare other observed variables such as cloud fraction, precipitation, boundary layer height, and radiative fluxes.

Thank you very much for this important comment. We agree that LWP alone is insufficient to fully evaluate the simulated cloud environment. Following the reviewer’s suggestion, we have clarified the definition of LWP and added additional observational constraints on the cloud radiative state and vertical structure.

First, we have revised the sentences in Sects. 2.1 (Lines 101-104), 2.2 (Lines 112-113), and 2.4 (Lines 174-176) to clarify the averaging method when calculating LWP. ERA5 LWP is scene-averaged, which is inherent to the dataset, whereas MODIS and WRF LWP represent cloudy (in-cloud) LWP. MODIS

retrievals are restricted to cloudy pixels, while WRF LWP is calculated for cloudy columns. Thus, MODIS and WRF LWP are consistent in definition and can be directly compared, whereas ERA5 provides an additional reference estimate of LWP.

(Lines 101-104): “In addition, several ERA5 variables are used during case screening and the evaluation of the simulated cloud evolution: CBH, total column liquid water (tclw; i.e., the scene-averaged LWP), and net solar radiation under all-sky and clear-sky conditions at both the top of the atmosphere (tsr, tsrc) and the surface (ssr, ssrc).”.

(Lines 112-113): “The observed LWP spatial distributions and temporal evolution are used to evaluate the WRF simulations. Note that MODIS LWP is retrieved for cloudy pixels only and thus represents cloudy (in-cloud) LWP.”

(Lines 174-176): “The WRF LWP is calculated only for cloud columns with QCLOUD $\geq 10^{-6}$ kg kg^{-1} at any model level and therefore also represents cloudy (in-cloud) LWP, consistent with the MODIS definition (Sect. 2.2). ”

In Sect. 3.1 (Lines 243-248 and 258-268), we further clarified the interpretation of d04 LWP and added comparisons of simulated SWCRE with CERES observations and CBH with CALIPSO observations. These additional comparisons provide observational constraints on the simulated cloud radiative state and vertical structure. We also clarified that the available coarse-resolution observations are insufficient to determine whether d04 agrees better with the “truth” than the coarser-resolution simulations.

(Lines 243-248): “To evaluate the meteorological background for Lagrangian transport, Fig. 1 shows the cloudy LWP distribution at 02:00 UTC on 24 September 2009. The d01 region exhibits a relatively homogeneous stratocumulus field, with a mean LWP of 136.11 g m^{-2} and a maximum of 346.66 g m^{-2}. As grid spacing decreases, finer-scale cloud structures and LWP variability become increasingly resolved, with d04 exhibiting a mean LWP of 86.65 g m^{-2} and a maximum of 632.13 g m^{-2}. These finer-scale structures provide more detailed representations of cloud and boundary-layer variability for subsequent parcel transport analysis.”

(Lines 258-268): “To evaluate the simulated cloud field and boundary-layer structure, Fig. 2 compares WRF LWP, SWCRE, and CBH with MODIS, CERES, CALIPSO, and ERA5. WRF d01 reproduces the observed increase in LWP from 23 to 24 September indicated by MODIS, whereas ERA5 shows the opposite trend (Figs. 2a, b). Although d04 captures the same trend as MODIS, its mean LWP is 43 – 44 % lower than that of WRF d01 sampled over the d04 region, highlighting substantial resolution sensitivity. However, the fine resolution and limited spatial coverage of the d04 domain limit direct comparisons with coarse-resolution satellite observations; model evaluation therefore focuses primarily on d01. The higher-resolution domains are primarily used to diagnose resolution-dependent turbulent parcel transport and cloud-base activation, rather than to demonstrate improved agreement with regional-mean observations. Both WRF and ERA5 slightly underestimate the magnitude of SWCRE (Fig. 2c). Both WRF and ERA5 also underestimate CBH relative to CALIPSO (Fig. 2d), with similar bias magnitudes for WRF d01 and ERA5. Overall, WRF captures the observed cloud evolution while

exhibiting resolution-dependent differences in cloud properties, providing a basis for investigating turbulent transport across grid spacings."

We have also added comparisons of low-cloud fraction and precipitation rate in Fig. R2. The WRF-simulated low-cloud fraction is generally lower than that from MODIS, and varies in a different temporal pattern with ERA5. Note that MODIS does not provide the temporal variations comparable to those in WRF and ERA5, so this comparison is of limited value. Rain rates from WRF, ERA5, and GPM remain near zero, consistent with the non-precipitating stratocumulus conditions in this case.

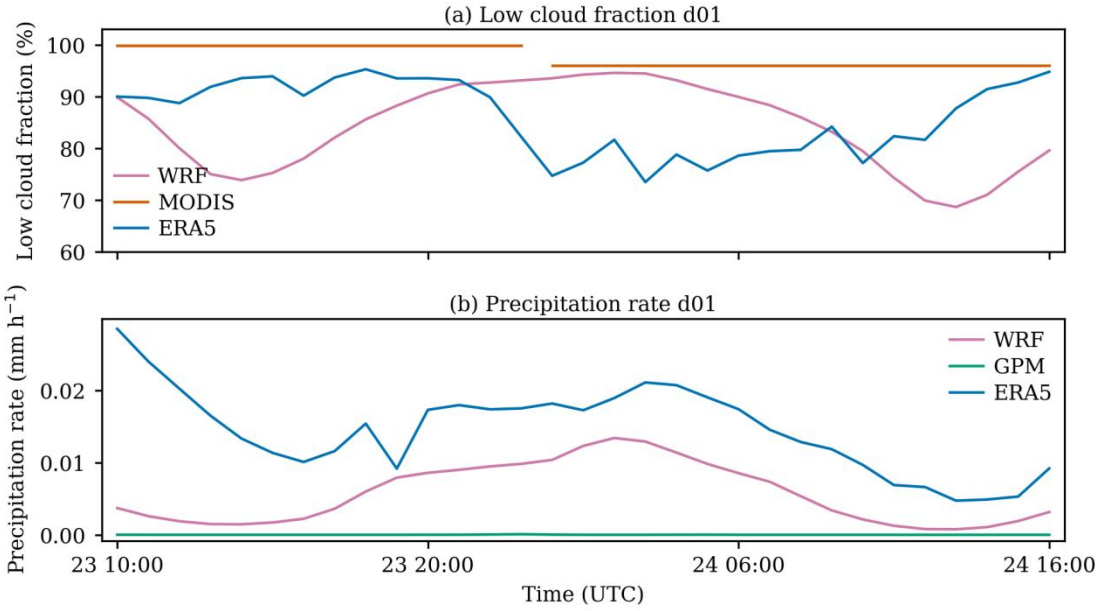


Figure R2. Temporal evolution over the clipped d01 region from 10:00 UTC on 23 September to 16:00 UTC on 24 September 2009. (a) Low cloud fraction (WRF, ERA5, and daily-mean MODIS); (b) Precipitation rate (WRF, ERA5, and GPM). The units of low cloud fraction and precipitation rate are % and mm h^{-1}, respectively. Colour conventions: WRF, ERA5, MODIS, and GPM are shown in reddish purple, blue, vermillion, and bluish green, respectively.

Notes:

To evaluate the simulated precipitation, we use the GPM IMERG Final Run half-hourly precipitation product (3B-HHR, V07B; Huffman et al., 2023), with a horizontal resolution of $0.1^{\circ}\times0.1^{\circ}$ and a temporal resolution of 30 min. The data cover the study period of 23–25 September 2009.

Since reliable PBLH observations with sufficient spatial and temporal correspondence to the study region and period were limited, we did not directly compare modeled and observed PBLH. Additionally, we selected this case by comparing ERA5 low cloud fraction with MODIS and choosing a focused period with strong consistency. WRF-simulated LWP, radiation, and cloud base height also generally agree with observations, indicating that the simulation is adequate for our analysis. Because our measurements are in coarse temporal and spatial resolution, assessing whether d04 agrees better with observations is not meaningful: agreement with the available observations does not demonstrate whether d04 is superior or not.

References:

Chen, J., Wang, H., Zhang, B., Liu, H., Painemal, D., Sorooshian, A., Tai, S.-L., and Voigt, C.: Response of marine post-frontal clouds to Gulf Stream variability, Atmos. Chem. Phys., 26, 2209–2224, https://doi.org/10.5194/acp-26-2209-2026 , 2026.

Cloux, S., Garaboa-Paz, D., Insua-Costa, D., Miguez-Macho, G., and Pérez-Muñuzuri, V.: Extreme precipitation events in the Mediterranean area: contrasting two different models for moisture source identification, Hydrol. Earth Syst. Sci., 25, 6465–6477, https://doi.org/10.5194/hess-25-6465-2021 , 2021.

Crespo-Otero, A., Insua-Costa, D., Hernández-García, E., López, C., and Míguez-Macho, G.: Simple physics-based adjustments reconcile the results of Eulerian and Lagrangian techniques for moisture tracking in atmospheric rivers, Earth Syst. Dynam., 16, 1483–1501, https://doi.org/10.5194/esd-16-1483-2025 , 2025.

Erfani, E., Wood, R., Blossey, P. N., Doherty, S. J., and Eastman, R.: Building a comprehensive library of observed Lagrangian trajectories for testing modeled cloud evolution, aerosol–cloud interactions, and marine cloud brightening, Atmos. Chem. Phys., 25, 8743–8768, https://doi.org/10.5194/acp-25-8743-2025, 2025.

Huffman, G. J., Stocker, E. F., Bolvin, D. T., Nelkin, E. J., Jackson, T., and Tan, J.: GPM IMERG Final Precipitation L3 Half Hourly 0.1 degree × 0.1 degree V07, Goddard Earth Sciences Data and Information Services Center (GES DISC), Greenbelt, MD, USA [data set], https://doi.org/10.5067/GPM/IMERG/3B-HH/07, 2023.

Kazemirad, M. and Miller, M. A.: Summertime post-cold-frontal marine stratocumulus transition processes over the eastern North Atlantic, J. Atmos. Sci., 77, 2011–2037, https://doi.org/10.1175/JAS-D-19-0167.1 , 2020.

McMichael, L. A., Schmidt, M., Wood, R., Blossey, P. N., and Patel, L.: Exploring ship track spreading rates with a physics-informed Langevin particle parameterization, Geoscientific Model Development, https://doi.org/10.5194/gmd-17-7867-2024, 2024.

McMichael, L. A., Erfani, E., Wood, R., and von Salzen, K.: Estimating Twomey forcing sensitivity to aerosol plume spreading rates, EGUsphere [preprint], https://doi.org/10.5194/ egusphere-2026-2730, 2026.

Prabhakaran, P., Hoffmann, F., and Feingold, G.: Effects of intermittent aerosol forcing on the stratocumulus-to-cumulus transition, Atmospheric Chemistry and Physics, https://doi.org/10.5194/acp-24-1919-2024, 2024.

Reviewer #2:

Review of Transport Efficiency of Turbulent Parcel in the Marine Boundary Layer and Its Implications for Droplet Activation in Marine Cloud Brightening

Authors: P. Zhao, J. Chen, Y. Yang, Y. Jia, and Y. Yu

General Comments

The introduction clearly explains the motivation and scientific relevance of the study and is generally well supported by previous literature. The combination of WRF and FLEXPART to investigate the full surface-to-cloud transport chain appears novel and promising. The tracking is based on passive tracers, but the consequences and limitations of this assumption are not sufficiently discussed. I encourage the authors to better justify these methodological choices and elaborate on their potential implications for the interpretation of the results. In addition, several parts of the discussion would be strengthened by a more comprehensive comparison with existing literature. The conclusions are frequently phrased in a general manner, although the analysis is based on a single case study. The authors should consistently distinguish case specific findings from general statements about MCB transport efficiency.

Thank you for these positive and constructive comments. We have revised the manuscript accordingly.

(1) We have expanded the discussion of the implications and limitations of the passive-tracer assumption in Sect. 2.5 (Lines 201-204): "The parcels are passive tracers without prescribed aerosol sizes or emission rates, which are considered separately in the activation analysis (Sect. 3.4). Thus, parcel counts represent numerical sampling rather than physical aerosol concentrations, and the diagnosed transport efficiency excludes aerosol-specific processes such as inertia, settling, deposition, and aerosol–meteorology interactions.".

We have further clarified the implications and limitations of the passive-tracer assumption in the conclusions (Lines 624-626): "Because FLEXPART-WRF tracks passive turbulent parcels without explicitly representing aerosol-specific processes, the diagnosed transport efficiency reflects air-parcel transport rather than actual aerosol delivery." We have also outlined potential directions for future research (Lines 626-628): "Future comparisons with passive-tracer simulations in WRF and with explicit aerosol/plume simulations using WRF-Chem could help distinguish uncertainties in turbulent transport from aerosol-specific effects.".

(2) Comparison with previous literature

The relevant literature and comparisons have been added to Sects. 3.2 (Lines 292-294, 306-310, and 314-316) and 3.3 (Lines 371-373 and 483-489).

(Lines 292-294): "To understand how varying meteorological conditions influence upward parcel transport across the 30 simulations, we examine the meteorological fields sampled along FLEXPART-WRF forward trajectories, focusing on the dynamical and thermodynamic processes governing marine stratocumulus-topped boundary layers (Wood, 2012; Ghate et al., 2015). "

(Lines 306-310): “This enhancement suggests that, in the early morning phase following the LWP maximum (at 02:00 UTC on the 24th), intensified longwave radiative cooling at cloud top drives vigorous vertical overturning, resulting in the strongest turbulent mixing within the cloud layer, consistent with the canonical view that nocturnal and early-morning stratocumulus turbulence is primarily maintained by cloud-top longwave radiative cooling and associated buoyancy production (Wood, 2012; Mellado, 2017).”

(Lines 314-316): “Such a moist mixed layer capped by a sharp inversion is characteristic of subtropical marine stratocumulus environments (Wood and Bretherton, 2004; Ghate et al., 2015). ”

(Lines 371-373): “This interpretation is consistent with previous LES studies showing that coherent updrafts can preferentially transport near-surface material toward cloud base and concentrate its delivery in space and time (Dhandapani et al., 2025). ”

(Lines 483-489): “The resolution dependence of parcel transport is consistent with previous LES studies highlighting the importance of resolved turbulent transport pathways for near-surface aerosol delivery (Dhandapani et al., 2025). Previous simulations and observations also demonstrate the roles of plume dispersion and meteorological conditions in transporting aerosols toward cloud base (McMichael et al., 2024; Kainz et al., 2026; Hernandez-Jaramillo et al., 2025). Although differences in transport metrics and experimental configurations preclude direct quantitative comparisons, our results are qualitatively consistent with these studies and provide complementary Lagrangian constraints on surface-to-cloud transport, without explicitly resolving aerosol dispersion or microphysical processes.”

(3) Case-specific conclusions and limitations

We have clarified the case-specific scope of the study in the conclusions (Lines 582-584): “This study investigates the transport of turbulent parcels from the ocean surface to the cloud base and its implications for cloud droplet activation in a Southeast Atlantic stratocumulus case. We decompose this pathway into the transport fraction reaching cloud base and the activation fraction from cloud-base aerosols to cloud droplets. ”

We have further addressed the limitation of the single-case analysis in the conclusions (Lines 623-624): “The analysis is limited to a single non-precipitating case, motivating future studies across broader regions, seasons, and meteorological conditions.”

Major Comments

- *Section 3.3 (L360 -...): The interpretation of the resolution sensitivity remains unclear. A substantial fraction of the diagnosed reduction in transport efficiency appears to arise from the cropped analysis domain and cut-off integration period, as acknowledged by the authors. (L374-375). It would be useful to more clearly separate physical resolution effects from methodological ones. Otherwise, readers may overinterpret the apparent resolution dependency as a robust physical result.*

Thank you for this helpful comment. We agree that the reduction in cumulative arrival rate should not be interpreted as a merely physical resolution effect. In the revised manuscript, we have revised the sentences in Lines 415-417, 419-423, and 434-440 to clarify it.

(Lines 415-417): "To ensure consistent cross-resolution comparisons, d02 and d03 are cropped to match the smaller d04 domain, and the analysis is limited to the first 90 min, during which at least 70 % of parcels remain within the domain across all release times, durations, and resolutions."

(Lines 419-423): "As the horizontal grid spacing decreases from d02 to d04, the peak instantaneous arrival rate decreases systematically for both release durations. For 10-min releases, the difference between the highest and lowest peak instantaneous arrival rates across the five release times decreases from 0.78 to 0.34 and 0.22 percentage points in d02, d03, and d04, respectively. For 60-min releases, this difference remains small across all three domains, ranging from 0.11 to 0.14 percentage points (Fig. 8, Table 3)."

(Lines 434-440): "The cumulative arrival rate quantifies parcel delivery to cloud base over time. For the 00:00 UTC release on 24 September, cumulative arrivals decrease from 96.02 % (d02) to 89.18 % (d03) and 83.35 % (d04) within the 90-min, d04-cropped framework (Fig. 8, Table 3). Extending the integration to 120 min and expanding the domain to d03 reduces the d02 – d03 differences from 3.03 – 11.59 to 2.25 – 7.93 percentage points across five release times and both release durations (Table 3). Unlike instantaneous quantities, the cumulative arrival rates reflect the combined effects of model resolution, domain size, and tracking duration, highlighting the importance of spatial and temporal sampling constraints when estimating aerosol delivery for MCB applications."

- *L395-397: I am confused by the interpretation of Figs. 10c-d. Figure 10c appears to show that the fraction of parcels embedded in a background ascending environment (f up) is generally largest for the highest-resolution simulation (d04), whereas the text states that this fraction decreases with increasing resolution. The figure seems to indicate a temporal decrease in f up (and corresponding increase in subsiding environments) for all simulations, but not a decrease with increasing resolution. Could the authors clarify this interpretation or revise the text?*

  Thank you for this comment. We have revised the text in Lines 446-449: "Figures 9c-d show that, within each simulation, the fraction of turbulent parcels embedded in background ascending environments generally decreases with time, whereas the fraction embedded in background subsiding environments increases. The ascending fraction is slightly higher in d04 than in d02 and d03 during most of the analysis period."

- *Section 3.4: you report AF of ~0.7-0.96 which could easily be interpreted as activation efficiencies of emitted particles. However, AF is conditioned on upward moving parcels that have already reached cloud base. The authors should more clearly distinguish this conditional activation metric from an overall aerosol activation efficiency and discuss how parcel transport and activation jointly determine the fraction of emitted particles that ultimately activate.*

  We have therefore revised Sect. 3.4 to state explicitly that AF is a conditional activation metric: "Here, AF is derived from cloud-base vertical velocities and represents the conditional activation

fraction of parcels reaching cloud base, rather than the overall activation efficiency of aerosols released near the ocean surface. FLEXPART-WRF is used solely to diagnose Lagrangian transport of turbulent air parcels, as no physical emission rate is prescribed (Sect. 2.5). Accordingly, cloud droplet activation is evaluated over a prescribed two-dimensional aerosol parameter space using the parameterization of Abdul-Razzak et al. (1998), rather than particle-derived three-dimensional concentration fields." in Lines 505-510.

Meanwhile, we have revised the sentences to explicitly describe AF as cloud-base activation fraction: "For parcels reaching cloud base, the conditional AF increases with increasing D_g and decreasing N_a (Fig. 11a), consistent with reduced critical supersaturation for larger aerosols and enhanced supersaturation under lower aerosol loading (e.g., Chen et al., 2018). AF shows little sensitivity to release duration (t_r = 60 min and t_r = 10 min in Fig. 11b), but is higher for releases at 00:00 than for those at 14:00 (Fig. 11c), likely due to stronger cloud-base updrafts during periods of higher LWP (Fig. 12). AF also increases systematically with horizontal resolution (Fig. 11d), with maximum values ranging from $0.76 – 0.91$ in d02 to $0.87 – 0.96$ in d03 and $0.93 – 0.96$ in d04. Similarly, mean AF across all 900 aerosol parameter combinations increases from $0.21 – 0.43$ in d02 to $0.32 – 0.50$ in d03 and $0.38 – 0.51$ in d04 (Table 4). This enhancement likely reflects stronger cloud-base updrafts resolved at finer grid spacing (Fig. 12b), although its magnitude depends on the prescribed aerosol conditions." in Lines 537-545.

To more explicitly discuss transport and activation, we introduce a joint transport-activation metric: "Because conditional AF represents only parcels reaching cloud-base activation conditions, it does not account for the fraction of surface-released aerosols that reach cloud base. Multiplying the fraction of transported parcels by the mean conditional AF yields approximate joint transport–activation fractions of $0.12 – 0.28$, $0.16 – 0.31$, and $0.18 – 0.32$ for d02, d03, and d04, respectively (Table 4). Although the joint fraction increases with resolution, it remains well below 0.5, highlighting that only a limited fraction of released aerosols may contribute to cloud droplet activation. These findings suggest caution when assuming that increased aerosol emissions translate directly into proportional increases in cloud droplet number concentration in MCB applications." (Lines 547-553).

Table 4 is added at lines 572-580 in the manuscript: "

Table 4. Summary of the transport-qualified fraction, mean conditional AF, and joint transport-activation metric for the five release times, three horizontal resolutions (d02, d03, and d04), and two release durations (t_r = 10 min and t_r = 60 min), based on a 90-min analysis period within the d04-cropped spatial domain. The transport-qualified fraction denotes the fraction of released turbulent parcels that reach the cloud-base activation layer and have positive vertical velocity at the first qualified point within the ±50 m layer. The mean conditional AF is averaged over the 900 prescribed (D_g , N_a) combinations. The joint metric is calculated as the product of the transport-qualified fraction and the mean conditional AF and is used as a diagnostic of the combined transport-activation pathway rather than as an absolute aerosol activation efficiency.

Domain	Release timing (UTC)	Transport-qualified fraction	Mean conditional AF	Joint metric	Transport-qualified fraction	Mean conditional AF	Joint metric
		t_r = 10 min			t_r = 60 min		
d02	23 14:00	0.55	0.21	0.12	0.48	0.24	0.12
	23 22:00	0.60	0.35	0.21	0.55	0.38	0.21
	24 00:00	0.71	0.40	0.28	0.58	0.39	0.23
	24 02:00	0.69	0.40	0.28	0.57	0.39	0.22
	24 06:00	0.59	0.43	0.25	0.54	0.40	0.22
d03	23 14:00	0.61	0.32	0.20	0.48	0.33	0.16
	23 22:00	0.59	0.45	0.27	0.52	0.46	0.24
	24 00:00	0.68	0.46	0.31	0.56	0.48	0.27
	24 02:00	0.66	0.47	0.31	0.52	0.47	0.24
	24 06:00	0.62	0.50	0.31	0.53	0.50	0.27
d04	23 14:00	0.61	0.38	0.23	0.47	0.39	0.18
	23 22:00	0.57	0.48	0.27	0.50	0.49	0.25
	24 00:00	0.67	0.48	0.32	0.54	0.49	0.26
	24 02:00	0.63	0.48	0.30	0.47	0.48	0.23
	24 06:00	0.57	0.51	0.29	0.47	0.50	0.24

".

- *L142: (1) what size of particles or undefined, (2) add reference for typical heights of MCB injection, (3) I think 50 000 is quite low number of particles being released. Typical MCB numbers are at least on the order of 1015 s-1 , this is only on the order of 10^3 (Wood et al. 2021). Are 50 000 parcels sufficient for statistical convergence of the transport diagnostics? A suggestion is to include a sensitivity test for a larger parcel ensemble, demonstrating this.*

  Thank you for this comment. We address the three points as follows.

  (1) Particle size.

  We have clarified this in the text:

  (Lines 194-195): "FLEXPART-WRF is run offline using archived WRF meteorological fields, with passive Lagrangian tracers released near the sea surface to represent turbulent air parcels rather than individual aerosol particles."

  (Lines 201-202): "The parcels are passive tracers without prescribed aerosol sizes or emission rates, which are considered separately in the activation analysis (Sect. 3.4). "

  (2) Typical MCB injection height.

  We have added references (Lines 198-200): "A total of 50 000 parcels (10 000 per box) are released from five regions at 0 – 20 m above the sea surface to represent turbulent air transport

near MCB sprayers. This configuration is consistent with previous FLEXPART-WRF and LES studies using near-surface releases (Cornwell et al., 2021; Salter et al., 2008; Kainz et al., 2026). ”

(3) Number of parcels and its relationship to the physical MCB emission rate.

We appreciate the reviewer’s concern regarding the number of released parcels. We agree that physical MCB aerosol production rates can be of order 10^{15} s^{-1}, as discussed in Wood (2021). However, the 50 000 parcels used in our simulations represent a numerical Lagrangian sampling ensemble, rather than a physical aerosol emission rate. FLEXPART-WRF is used here in passive-parcel mode to characterize turbulent transport from the near-surface marine environment to cloud base. Thus, the number of numerical parcels and the physical aerosol production rate represent different quantities and should not be directly compared.

Our use of parcel ensembles is also consistent with previous LES-driven FLEXPART-WRF applications. For example, Cornwell et al. (2021) used 10 000 inert tracers in each FLEXPART-WRF sensitivity experiment to diagnose turbulent transport. In our study, 50 000 parcels are distributed among five spatially separated release regions (10 000 per box) to sample near-surface turbulent transport.

To assess the sensitivity of the transport diagnostics to parcel number, we conducted additional experiments using ensembles of 1 000, 2 000, 5 000, 10 000, 20 000, 50 000, and 100 000 parcels for the 00:00 UTC release on 24 September in d02, with an analysis period of 180 min (t_r = 10 min). The final cumulative arrival rates remain highly consistent across the tested ensemble sizes, ranging from 99.80 % to 99.88 %. These results indicate that the final cumulative arrival rate is insensitive to parcel number under the tested configuration, providing evidence that the 50 000-parcel ensemble is sufficient for this diagnostic in the selected case.

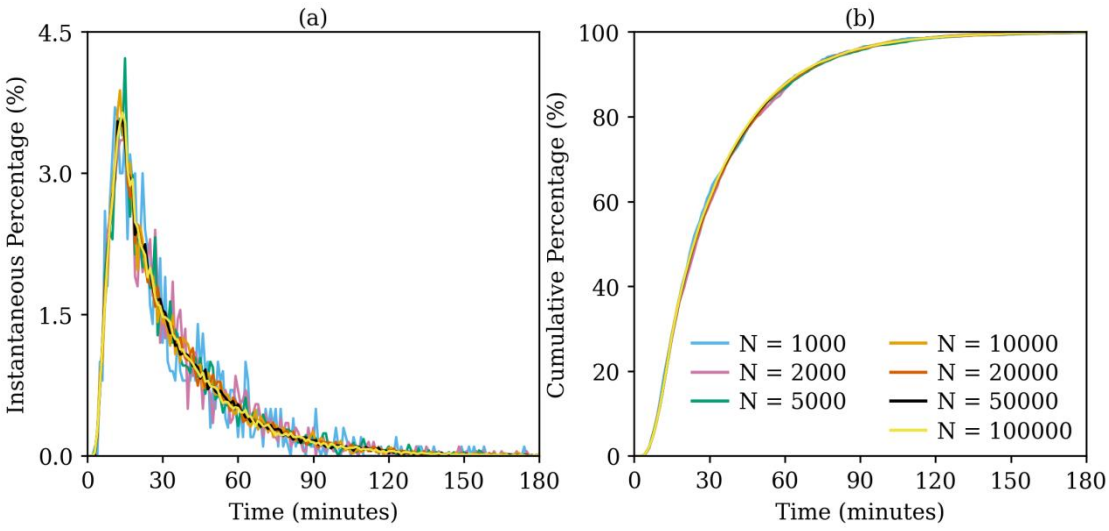


Figure R3. Sensitivity of the instantaneous and cumulative parcel arrival rates to the total number of released air parcels (N) in the d02 simulation initialized at 00:00 UTC on 24 September 2009, with a release duration of t_r = 10 min and an analysis period of 180 min. (a) Instantaneous arrival rate, (b) cumulative arrival rate. Arrival rates are expressed as percentages of the total number of parcels released in each experiment. The curves represent 1 000 (sky blue), 2 000 (reddish purple), 5 000 (bluish green), 10 000 (orange), 20 000 (vermillion), 50 000 (black), and 100 000 (yellow).

Table R1. Peak instantaneous arrival rate, time of peak arrival rate, and final cumulative arrival rate for different total numbers of released air parcels in the d02 sensitivity experiments (release at 00:00 UTC on 24 September 2009, t_r = 10 min, 180-min analysis period).

Domain	Release timing (UTC)	Parcel number	Analysis period	Peak (%)	Peak Time (min)	Final cumulative (%)
d02	24 00:00	1000	180	3.70	11	99.80
d02	24 00:00	2000	180	3.40	15	99.85
d02	24 00:00	5000	180	4.22	15	99.84
d02	24 00:00	10000	180	3.88	13	99.86
d02	24 00:00	20000	180	3.50	13	99.88
d02	24 00:00	50000	180	3.60	14	99.83
d02	24 00:00	100000	180	3.64	14	99.86

- *Section 3.1: Although the model evaluation provides useful context, this subsection feels disproportionately long given that it is not directly tied to the main research questions. The analysis effectively introduces an additional research question regarding the relative skill of WRF, ERA5, and MODIS in representing stratocumulus and LWP. I suggest streamlining this section and moving some of the supporting figures or discussion to the Appendix. Furthermore, this result is highlighted as a main finding, despite not being one of the primary questions posed by the study.*

  Thank you for this comment. We agree that the model evaluation is not itself one of the primary research questions; rather, a concise evaluation is a necessary basis for this study, because all subsequent Lagrangian transport and activation diagnostics rely on the credibility of the simulated cloud and boundary-layer environment. We also note that Reviewer #1 explicitly requested observational comparisons beyond LWP. In the revision, we have consolidated the observational evaluation into a single multi-variable figure (Fig. 2) with a compact discussion, so that the section remains concise without requiring an appendix (Lines 243-248 and 258-289). We have removed the model-evaluation results as a standalone main finding.

  (Lines 243-248): "To evaluate the meteorological background for Lagrangian transport, Fig. 1 shows the cloudy LWP distribution at 02:00 UTC on 24 September 2009. The d01 region exhibits a relatively homogeneous stratocumulus field, with a mean LWP of 136.11 g m^{-2} and a maximum of 346.66 g m^{-2}. As grid spacing decreases, finer-scale cloud structures and LWP variability become increasingly resolved, with d04 exhibiting a mean LWP of 86.65 g m^{-2} and a maximum of 632.13 g m^{-2}. These finer-scale structures provide more detailed representations of cloud and boundary-layer variability for subsequent parcel transport analysis."

  (Lines 258-289): "To evaluate the simulated cloud field and boundary-layer structure, Fig. 2 compares WRF LWP, SWCRE, and CBH with MODIS, CERES, CALIPSO, and ERA5. WRF d01 reproduces the observed increase in LWP from 23 to 24 September indicated by MODIS, whereas ERA5 shows the opposite trend (Figs. 2a, b). Although d04 captures the same trend as MODIS, its mean LWP is 43 – 44 % lower than that of WRF d01 sampled over the d04 region, highlighting substantial resolution sensitivity. However, the fine resolution and limited spatial coverage of the d04 domain limit direct comparisons with coarse-resolution satellite observations; model evaluation therefore focuses primarily on d01. The higher-resolution domains are primarily

used to diagnose resolution-dependent turbulent parcel transport and cloud-base activation, rather than to demonstrate improved agreement with regional-mean observations. Both WRF and ERA5 slightly underestimate the magnitude of SWCRE (Fig. 2c). Both WRF and ERA5 also underestimate CBH relative to CALIPSO (Fig. 2d), with similar bias magnitudes for WRF d01 and ERA5. Overall, WRF captures the observed cloud evolution while exhibiting resolution-dependent differences in cloud properties, providing a basis for investigating turbulent transport across grid spacings.

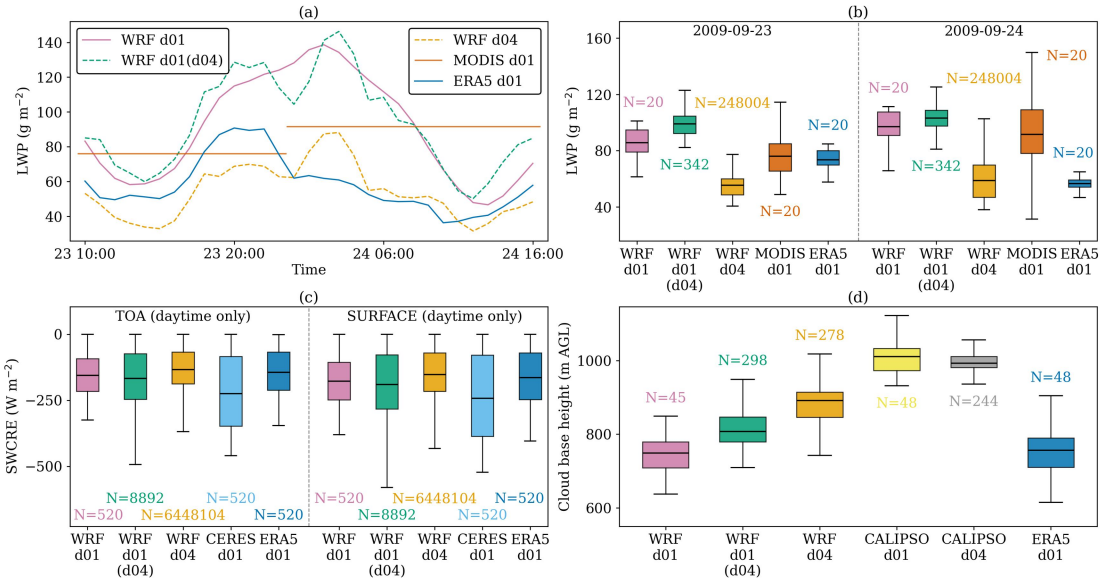


Figure 2. Comparison of cloud and boundary-layer characteristics between WRF simulations, ERA5 reanalysis, and satellite observations. (a) Temporal evolution of LWP from 10:00 UTC on 23 September to 16:00 UTC on 24 September 2009. WRF d01, WRF d01(d04) (i.e., WRF d01 clipped to the d04 region), and WRF d04 are 1-hour averages, ERA5 provides hourly data, and MODIS provides daily means. (b) Boxplots of daily-mean LWP for 23 – 24 September. WRF d01 and ERA5 are matched to a 1° grid, WRF d01(d04) and WRF d04 retain their native grids, and MODIS is provided on its native 1° daily grid. (c) Boxplots of 1-hour mean TOA and surface SWCRE during daytime on 23 – 24 September, with data over the d01 region uniformly matched to a 1° grid, while WRF d01(d04) and WRF d04 retain their native grids. (d) Boxplots of CBH during two CALIPSO overpasses (01:47:38 and 14:06:05 UTC) on 23 September 2009; no CALIPSO data are available over the entire d01 region on 24 September. For the d01 region, CALIPSO, WRF, and ERA5 data are matched to a 0.25° grid, whereas for the d04 region, WRF d01 and WRF d04 are interpolated along the CALIPSO track to the original footprint locations. For both regions, ERA5 and WRF data are temporally matched to the CALIPSO overpass times with the corresponding spatial matching procedures. In the boxplots, boxes represent the interquartile range (IQR), and black horizontal lines indicate means; the corresponding statistics and sample size N are labeled adjacent to each box. In panel (a), WRF d01 (solid line), WRF d01(d04) (dashed line), WRF d04 (dashed line), MODIS d01 (solid line), and ERA5 d01 (solid line) are compared. Colors are kept consistent throughout the figure: WRF d01, WRF d01(d04), WRF d04, MODIS d01, ERA5 d01, CERES d01, CALIPSO d01, and CALIPSO d04 are shown in reddish purple, bluish green, orange, vermillion, blue, sky blue, yellow, and grey, respectively. All d01 data are extracted from the clipped region (14.65°S – 10.00°S, 10.00°W – 5.70°W; Fig. 1a)."

- *Discussion: generally, you do not interpret or link the results to other literature on transport of particles through the lower atmosphere. It would benefit from a more explicit comparison of the reported efficiencies with previous LES studies of aerosol plume transport and MCB relevant aerosol delivery.*

We have expanded Sects. 3.2 (Lines 292-294, 306-310, and 314-316) and 3.3 (Lines 371-373 and 483-489) to discuss our findings with previous studies of turbulent transport, near-surface material delivery, and aerosol transport relevant to MCB. The added text has been showed below.
The relevant literature and comparisons have been added to Sects. 3.2 (Lines 292-294, 306-310, and 314-316) and 3.3 (Lines 371-373 and 483-489).

(Lines 292-294): "To understand how varying meteorological conditions influence upward parcel transport across the 30 simulations, we examine the meteorological fields sampled along FLEXPART-WRF forward trajectories, focusing on the dynamical and thermodynamic processes governing marine stratocumulus-topped boundary layers (Wood, 2012; Ghate et al., 2015). "

(Lines 306-310): "This enhancement suggests that, in the early morning phase following the LWP maximum (at 02:00 UTC on the 24th), intensified longwave radiative cooling at cloud top drives vigorous vertical overturning, resulting in the strongest turbulent mixing within the cloud layer, consistent with the canonical view that nocturnal and early-morning stratocumulus turbulence is primarily maintained by cloud-top longwave radiative cooling and associated buoyancy production (Wood, 2012; Mellado, 2017)."

(Lines 314-316): "Such a moist mixed layer capped by a sharp inversion is characteristic of subtropical marine stratocumulus environments (Wood and Bretherton, 2004; Ghate et al., 2015). "

(Lines 371-373): "This interpretation is consistent with previous LES studies showing that coherent updrafts can preferentially transport near-surface material toward cloud base and concentrate its delivery in space and time (Dhandapani et al., 2025). "

(Lines 483-489): "The resolution dependence of parcel transport is consistent with previous LES studies highlighting the importance of resolved turbulent transport pathways for near-surface aerosol delivery (Dhandapani et al., 2025). Previous simulations and observations also demonstrate the roles of plume dispersion and meteorological conditions in transporting aerosols toward cloud base (McMichael et al., 2024; Kainz et al., 2026; Hernandez-Jaramillo et al., 2025). Although differences in transport metrics and experimental configurations preclude direct quantitative comparisons, our results are qualitatively consistent with these studies and provide complementary Lagrangian constraints on surface-to-cloud transport, without explicitly resolving aerosol dispersion or microphysical processes."

Minor Comments

- *L46-48: authors should support claim with literature.*

  We have added relevant references. The revised text is provided below (Lines 45-50):
  "Although previous studies have largely relied on Eulerian diagnostics of plume evolution and cloud responses (Wang et al., 2011; Jenkins and Forster, 2013; Jenkins et al., 2013; Maalick et al., 2014; Chun et al., 2023), Lagrangian approaches can track trajectories by following near-surface-to-cloud-base transport pathways and linking them to cloud evolution and aerosol–cloud interactions (Erfani et al., 2025). As a result, the dynamical pathways linking

surface release to cloud-base arrival and subsequent activation remain insufficiently quantified from a Lagrangian perspective."

- *L84: authors are advised to include a concise paragraph that outlines the chain of datasets used to set up your simulations and explained thereafter. The reanalysis dataset comes out of the blue. Or move L90-91 (ERA5 serves…) to beginning paragraph. Also, introduce that you use WRF in LES mode as the LES model. This would improve readibility for readers that are less familiar with the used model setup.*

  We have added a concise overview at the beginning of Sect. 2 to outline the workflow connecting the datasets and models used in this study. The revised text is provided below (Lines 86-93):

  "This section describes the model configurations and datasets used in this study. Case selection is based on the agreement in low-cloud fraction between ERA5 and MODIS. The selected case is then simulated using WRF version 4.6, with ERA5 providing the initial and lateral boundary conditions and a nested configuration spanning horizontal grid spacings from 2.7 km to 100 m (Sect. 2.4). Model evaluation uses MODIS cloudy liquid water path (LWP), CERES shortwave cloud radiative effect (SWCRE), and CALIPSO/CALIOP cloud base height (CBH), with ERA5 providing additional reference estimates of CBH, LWP, and SWCRE at the top of the atmosphere and the surface. Finally, FLEXPART-WRF is driven by the simulated WRF meteorological fields to diagnose turbulent parcel transport (Sect. 2.5). Further details are provided in the following subsections."

- *L109-111: do you specifically filter for low clouds or cloud presence in general, could you comment on that?*

  We filtered for low clouds. The revised text is provided below (Lines 144-149):

  "We select a case where the low cloud fraction from the ERA5 reanalysis closely matches MODIS observations, thereby increasing confidence in the meteorological forcing field. Specifically, during the simulation period from 23 to 25 September, the ERA5 low cloud fractions are 56.90 %, 57.52 %, and 52.43 %, respectively, which exhibit good agreement with the MODIS observations of 57.28 %, 57.32 %, and 56.72 %. The consistency between ERA5 and MODIS low cloud fractions on 23 and 24 September justifies the selection of this period for analysis of parcel transport with a realistically represented stratocumulus cloud environment. "

- *L117: I would argue that 100m is on the higher end of what a LES resolution should have, or no no bigger then 300m. Overall, you would expect the LWP to perform better for higher resolution, but this doesn't appear so in Figure 2. In combination with later limitations of such a small domain in the analysis, authors are advised to either look in the performance in more detail or suggest omitting.*

  We agree that the 100 m grid spacing of d04 is at the coarse end of LES resolutions. We have clarified the role of the nested domains in Lines 157-160: "Of the inner domains, only the 100 m grid spacing of d04 falls within the range typically used for boundary-layer LES, whereas the 900 m (d02) and 300 m (d03) grids span the transition toward this regime; the nested d02 – d04 design is therefore used to quantify the sensitivity of the diagnosed parcel transport and cloud-base activation to grid spacing (Sects. 3.3 – 3.4)."

Regarding the LWP comparison, we added comparisons of LWP, SWCRE, and CBH with MODIS, CERES, and CALIPSO, respectively, in Sect. 3.1 (Lines 258-268): “To evaluate the simulated cloud field and boundary-layer structure, Fig. 2 compares WRF LWP, SWCRE, and CBH with MODIS, CERES, CALIPSO, and ERA5. WRF d01 reproduces the observed increase in LWP from 23 to 24 September indicated by MODIS, whereas ERA5 shows the opposite trend (Figs. 2a, b). Although d04 captures the same trend as MODIS, its mean LWP is 43 – 44 % lower than that of WRF d01 sampled over the d04 region, highlighting substantial resolution sensitivity. However, the fine resolution and limited spatial coverage of the d04 domain limit direct comparisons with coarse-resolution satellite observations; model evaluation therefore focuses primarily on d01. The higher-resolution domains are primarily used to diagnose resolution-dependent turbulent parcel transport and cloud-base activation, rather than to demonstrate improved agreement with regional-mean observations. Both WRF and ERA5 slightly underestimate the magnitude of SWCRE (Fig. 2c). Both WRF and ERA5 also underestimate CBH relative to CALIPSO (Fig. 2d), with similar bias magnitudes for WRF d01 and ERA5. Overall, WRF captures the observed cloud evolution while exhibiting resolution-dependent differences in cloud properties, providing a basis for investigating turbulent transport across grid spacings.”

D04 provides finer-scale dynamical information for examining cloud-base updrafts and their effects on turbulent parcel transport and activation-relevant processes. We also acknowledge that the small d04 domain and 90 min analysis period lead to lateral parcel loss and limit cross-resolution comparisons for cumulative quantities; the associated limitations and future-work directions are discussed in Sect. 4 (Line 628): “Larger or periodic domains could reduce lateral parcel loss and sampling limitations”

- *Section 2.4/2.5: for readabiltiy, please omit settings like ra_sw_physics = 4 in main text, include a table with experimental overview in methods (or partially Appendix).*

  In the revised manuscript, we removed these detailed option-value listings from Sects. 2.4 and 2.5 and added Tables 1-2 in the Methods section to provide a concise overview of the main WRF and FLEXPART-WRF configurations and experimental settings used in this study (Lines 233-239).

Table 1. Main WRF and FLEXPART-WRF configurations used in this study.

Model	Option	Setting	Description
WRF	mp_physics	8	Thompson microphysics scheme
	ra_sw_physics	4	RRTMG shortwave radiation scheme
	ra_lw_physics	4	RRTMG longwave radiation scheme
	sf_sfclay_physics	2	Monin-Obukhov (Janjic Eta) surface layer scheme
	sf_surface_physics	2	Noah land surface model
	bl_pbl_physics	2 (d01), 0 (d02 – d04)	MYJ PBL scheme in d01; no PBL scheme in inner domains (d02 – d04)
	history_interval	15 (d01), 1 (d02 – d04)	Output interval in minutes
FLEXPART-WRF	TURB_OPTION	1	Turbulence diagnosed as in FLEXPART-ECMWF
	WIND_OPTION	-1	Vertical velocity derived from mass-consistent horizontal wind divergence
	SFC_OPTION	0	Default computation of friction velocity, surface heat flux, and PBL height
	CBL_SCHEME	1	Skewed-turbulence scheme for the convective boundary layer
	source regions	5 boxes	Five release boxes in the southeastern corner of the domain
	parcel number	50 000	Total number of released parcels
	release height	0 – 20 m	Near-surface release layer

Table 2. Overview of the 30 FLEXPART-WRF parcel-release experiments.

Domain	Release timing (UTC)	Release duration (min)
d02	23 14:00	10
	23 14:00	60
	23 22:00	10
	23 22:00	60
	24 00:00	10
	24 00:00	60
	24 02:00	10
	24 02:00	60
	24 06:00	10
	24 06:00	60
d03	23 14:00	10
	23 14:00	60
	23 22:00	10
	23 22:00	60
	24 00:00	10
	24 00:00	60
	24 02:00	10
	24 02:00	60
	24 06:00	10
	24 06:00	60
d04	23 14:00	10
	23 14:00	60
	23 22:00	10
	23 22:00	60
	24 00:00	10
	24 00:00	60
	24 02:00	10
	24 02:00	60
	24 06:00	10
	24 06:00	60

- *(2) Release timing. How do you account for the carry-over effects of previous releases on later CDNC perturbations? Or do you have separate simulations for each release time? Please clarify and include a Table with experimental overview.*

  We conduct separate simulations for each release time, with no carry-over effects between releases. Note that FLEXPART-WRF is a post-processing tool driven by WRF output. We have clarified this in Lines 214-218 and added an overview of the 30 experiments in Table 2.

  (Lines 214-218): "These release times sample different stages of cloud development to assess transport variability under evolving meteorological conditions. Each release time-duration combination is simulated independently using offline FLEXPART-WRF, with passive tracers that do not affect WRF meteorology or cloud properties. Cloud droplet activation is diagnosed separately in post-processing (Sect. 3.4), ensuring no carry-over effects between experiments."

Table 2. Overview of the 30 FLEXPART-WRF parcel-release experiments.

Domain	Release timing (UTC)	Release duration (min)
d02	23 14:00	10
	23 14:00	60
	23 22:00	10
	23 22:00	60
	24 00:00	10
	24 00:00	60
	24 02:00	10
	24 02:00	60
	24 06:00	10
	24 06:00	60
d03	23 14:00	10
	23 14:00	60
	23 22:00	10
	23 22:00	60
	24 00:00	10
	24 00:00	60
	24 02:00	10
	24 02:00	60
	24 06:00	10
	24 06:00	60
d04	23 14:00	10
	23 14:00	60
	23 22:00	10
	23 22:00	60
	24 00:00	10
	24 00:00	60
	24 02:00	10
	24 02:00	60
	24 06:00	10
	24 06:00	60

- *L465: What do the authors mean with moving upward under the prescribed aerosol conditions. Could the authors explain, do you mean L477-478?*

  We have removed the confusing wordings and added the relevant clarifications to the revised manuscript (Lines 505-506 and 520-524).

  (Lines 505-506): “Here, AF is derived from cloud-base vertical velocities and represents the conditional activation fraction of parcels reaching cloud base, rather than the overall activation efficiency of aerosols released near the ocean surface.”

  (Lines 520-524): “ For each trajectory, the first point at which RH exceeds 100 % is identified as the reference level for the cloud-base activation layer, which extends 50 m above and below this level. A trajectory is classified as transport-qualified if a positive vertical velocity ($w > 0$) occurs within this layer, and the first such point is then used for the subsequent AF calculation. This procedure ensures that AF is evaluated only for parcels that both reach the cloud-base region and have upward motion favorable for activation.”

- *L473: suggestion for the authors to add background to aerosol number concentration (if that is what you mean, which I suppose) or is it not? If it's not, do you mean that you exclude all the information from the cloud-base particle number and residence time fully in this analysis? Please clarify and consider including this key information in your activation analysis.*

  This comment raises two related points. We address both and have revised Sect. 2.5 and Sect. 3.3-3.4 accordingly.

  (1) Yes, N_a denotes the aerosol number concentration. In the revised Sect. 3.4 we now state that (Lines 516-517) "the aerosol number concentration (N_a) ranges from $10 – 5000\ cm^{-3}$, representing both clean and polluted marine environments (Quinn et al., 2017; O'Dowd and de Leeuw, 2007).". At the same time, N_a is a prescribed, idealized input parameter of a 30×30 (D_g, N_a) parameter space, not a concentration field derived from the FLEXPART-WRF parcel positions. As stated in Sect. 2.5 (Lines 201-204): "The parcels are passive tracers without prescribed aerosol sizes or emission rates, which are considered separately in the activation analysis (Sect. 3.4). Thus, parcel counts represent numerical sampling rather than physical aerosol concentrations, and the diagnosed transport efficiency excludes aerosol-specific processes such as inertia, settling, deposition, and aerosol–meteorology interactions.". Sect. 3.4 is explicit (Lines 507-510): "FLEXPART-WRF is used solely to diagnose Lagrangian transport of turbulent air parcels, as no physical emission rate is prescribed (Sect. 2.5). Accordingly, cloud droplet activation is evaluated over a prescribed two-dimensional aerosol parameter space using the parameterization of Abdul-Razzak et al. (1998), rather than particle-derived three-dimensional concentration fields.".

  (2) Cloud-base particle number and residence time are not excluded—they are considered in the different part of analysis.

  Cloud-base transport is included: the AF calculation is applied only to parcels that actually reach cloud base and move upward there. Sect. 3.4 (Lines 520-524): "For each trajectory, the first point at which RH exceeds 100 % is identified as the reference level for the cloud-base activation layer, which extends 50 m above and below this level. A trajectory is classified as transport-qualified if a positive vertical velocity ($w > 0$) occurs within this layer, and the first such point is then used for the subsequent AF calculation. This procedure ensures that AF is evaluated only for parcels that both reach the cloud-base region and have upward motion favorable for activation.".

  The effect of transportation is also quantified jointly with AF: Sect. 3.4 (Lines 547-550): "Because conditional AF represents only parcels reaching cloud-base activation conditions, it does not account for the fraction of surface-released aerosols that reach cloud base. Multiplying the fraction of transported parcels by the mean conditional AF yields approximate joint transport–activation fractions of $0.12 – 0.28$, $0.16 – 0.31$, and $0.18 – 0.32$ for d02, d03, and d04, respectively (Table 4).".

  In-cloud residence time is diagnosed separately as a transport characteristic (Sect. 3.3) but is not incorporated into the present activation parameterization. We identify this as a direction for future

work in Sect. 4 (Lines 629-630): “cloud parcel model simulations that resolve supersaturation and droplet growth over the in-cloud residence time”.

- *Suggestion: Rename Results to Results and Discussion*

  We have renamed the section from “Results” to “Results and Discussion” in the revised manuscript (Line 241).

- *Suggestion: Include Equation 30 of Abdul Razzak because it is the foundation of all your activation results.*

  We have added this equation explicitly in Sect. 3.4 of the revised manuscript while retaining the citation to the original source (Lines524-531):

  “The sampled variables within the activation height range are then used to compute the activation fraction following Eq. (30) of Abdul-Razzak et al. (1998), written here as

$$\frac{N}{N_{ap}} = \frac{1}{2}\operatorname{erfc}\left\{\ln\left[f_1(\ln\sigma)\left(\frac{\zeta}{\eta}\right)^{\frac{3}{2}} + f_2(\ln\sigma)\left(\frac{S_m^2}{\eta+3\zeta}\right)^{\frac{3}{4}}\right] \div (3\sqrt{2}\ln\sigma)\right\} \#(1)$$

  where N/N_{ap} gives the conditional AF, N is the activated aerosol number concentration, N_{ap} is the total aerosol number concentration, S_m is the critical supersaturation corresponding to the geometric mean diameter, σ is the geometric standard deviation of the aerosol size distribution, and f_1, f_2, η, and ζ are defined following Abdul-Razzak et al. (1998).”

Technical Corrections

- *Abstract: omit d02 full or more explanatory name*

  We have revised Lines 23-25 to provide the full descriptive names at first mention and retain the shorthand labels thereafter: “For parcels released at 00:00 UTC on 24 September (t_r = 10 min), the peak instantaneous arrival rate decreases from 3.60 % in the 900 m grid-spacing domain (d02) to 2.04 % in the 100 m grid-spacing domain (d04)”.

- *L167: some lay out issue with the 10-6 kg/kg*

  We checked the layout of this expression and standardized its formatting in the revised manuscript. The threshold remains unchanged (Line 221): “10^{-6} kg kg^{-1}”

- *L181: formatting units LWP unequal*

  This has been revised on Line 252: “**g m^{-2}**”

- *L184: formatting of coordinates not in bold*

  This has been revised on Line 289: “**14.65°S – 10.00°S, 10.00°W – 5.70°W**”

- *Fig 2: clarify contrast between day 23 or day 24 and time this is unclear*

We have substantially revised Fig. 2 to improve the clarity of the temporal information and the presentation of the different variables, datasets, and spatial and temporal sampling procedures. The revised caption also provides detailed descriptions of the time periods, spatial matching, and data processing for each panel (Lines 273-289):

"**Figure 2. Comparison of cloud and boundary-layer characteristics between WRF simulations, ERA5 reanalysis, and satellite observations. (a) Temporal evolution of LWP from 10:00 UTC on 23 September to 16:00 UTC on 24 September 2009. WRF d01, WRF d01(d04) (i.e., WRF d01 clipped to the d04 region), and WRF d04 are 1-hour averages, ERA5 provides hourly data, and MODIS provides daily means. (b) Boxplots of daily-mean LWP for 23 – 24 September. WRF d01 and ERA5 are matched to a 1° grid, WRF d01(d04) and WRF d04 retain their native grids, and MODIS is provided on its native 1° daily grid. (c) Boxplots of 1-hour mean TOA and surface SWCRE during daytime on 23 – 24 September, with data over the d01 region uniformly matched to a 1° grid, while WRF d01(d04) and WRF d04 retain their native grids. (d) Boxplots of CBH during two CALIPSO overpasses (01:47:38 and 14:06:05 UTC) on 23 September 2009; no CALIPSO data are available over the entire d01 region on 24 September. For the d01 region, CALIPSO, WRF, and ERA5 data are matched to a 0.25° grid, whereas for the d04 region, WRF d01 and WRF d04 are interpolated along the CALIPSO track to the original footprint locations. For both regions, ERA5 and WRF data are temporally matched to the CALIPSO overpass times with the corresponding spatial matching procedures. In the boxplots, boxes represent the interquartile range (IQR), black horizontal lines indicate means; the corresponding statistics and sample size N are labeled adjacent to each box. In panel (a), WRF d01 (solid line), WRF d01(d04) (dashed line), WRF d04 (dashed line), MODIS d01 (solid line), and ERA5 d01 (solid line) are compared. Colors are kept consistent throughout the figure: WRF d01, WRF d01(d04), WRF d04, MODIS d01, ERA5 d01, CERES d01, CALIPSO d01, and CALIPSO d04 are shown in reddish purple, bluish green, orange, vermillion, blue, sky blue, yellow, and grey, respectively. All d01 data are extracted from the clipped region (14.65°S – 10.00°S, 10.00°W – 5.70°W; Fig. 1a).**"

- *L239: specific humidity to water vapor specific humidity*

We have corrected "specific humidity" to "water vapor specific humidity" in the revised manuscript (Line 296).

- *Formatting issues in caption figure 4, 5*

In the revised manuscript the original Figs. 4 and 5 have been renumbered as Figs. 3 and 4, respectively. We have also corrected the formatting issues in their captions (Lines 344-348 and 351-353).

(Lines 344-348): **"Figure 3. Vertical profiles of background meteorological parameters for turbulent parcels at different release times (t_r = 10 min, trajectory duration 180 min). (a-c) q_v,θ, and TKE in the supersaturated region (RH > 100%). (d-f) corresponding parameters in the unsaturated region (RH < 100%). Colors indicate different times, including blue (14:00 UTC on the 23rd), reddish purple (22:00 UTC on the 23rd), black (00:00 UTC on the 24th), vermillion (02:00 UTC on the 24th), and bluish green (06:00 UTC on the 24th). Shading represents ±1σ. The unit of q_v is g kg^{-1}. The unit of θ is K. The unit of TKE is m^2 s^{-2}."**

(Lines 351-353): **"Figure 4. KDE distributions of q_v and θ as a function of height for the representative times (14:00 UTC on the 23rd and 02:00 UTC on the 24th). The upper panels show the supersaturated region (RH > 100%), and the lower panels show the unsaturated region (RH < 100%). N denotes the statistical sample size. The unit of q_v is g kg^{-1}. The unit of θ is K."**

- *L247: insert space between 11 and g*

We have inserted the missing space between "11" and "g" in the revised manuscript (Line 303): "9.00 – 10.87 g kg^{-1}"

- *Fig 7: y-axis of (a) needs to include instantaneous*

In the revised manuscript the original Fig. 7 has been renumbered as Fig. 6 (and the original Fig. 9 as Fig. 8). We have updated the y-axis labels of Fig. 6a and Fig. 8a to explicitly include "instantaneous" (Lines 393 and 424).

Fig. 6:

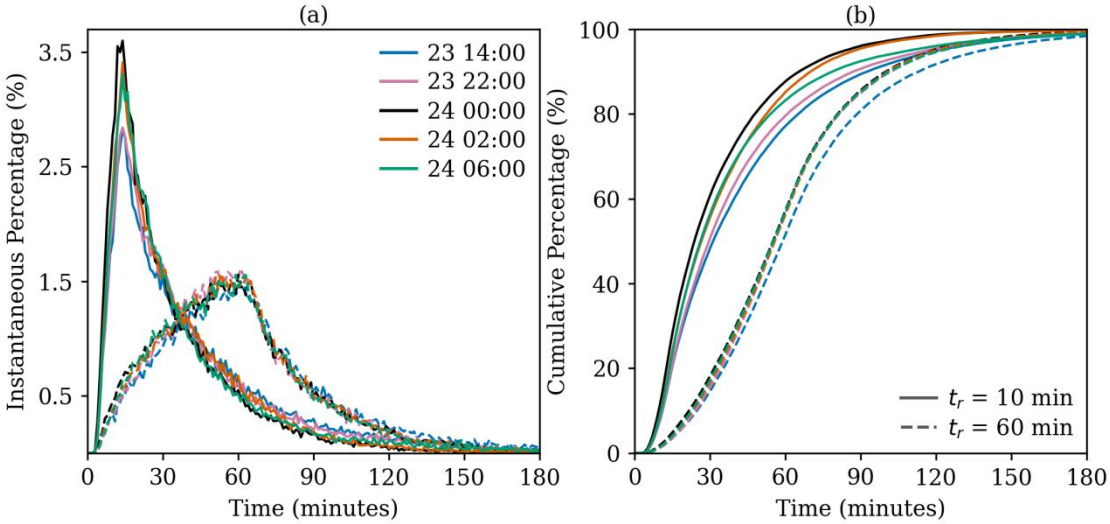
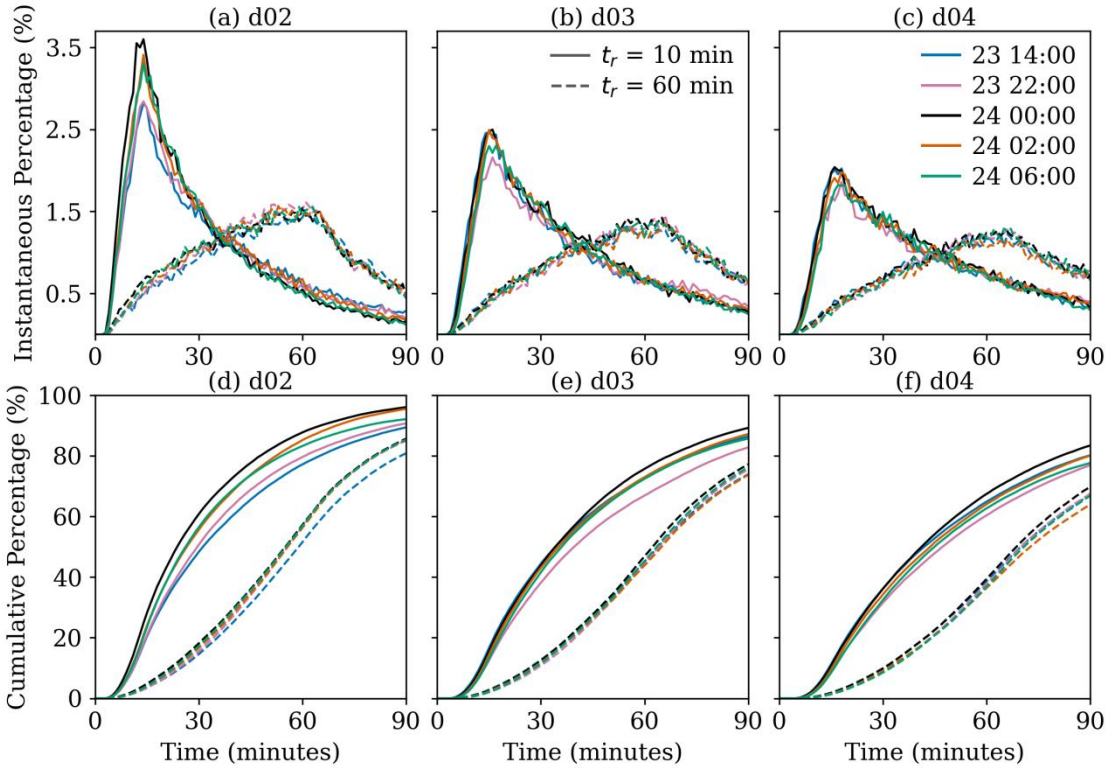


Fig. 8:



- *Fig 8 title: clarify contrast between day 23 or day 24 and time this is unclear*

In the revised manuscript the original Fig. 8 has been renumbered as Fig. 7 (and the original Fig. 11 as Fig. 10). We have revised the panel titles in Fig. 7 to clearly indicate the date and UTC time, and we have made the corresponding revision in Fig. 10 for consistency (Lines 402 and 491).

Fig. 7 :

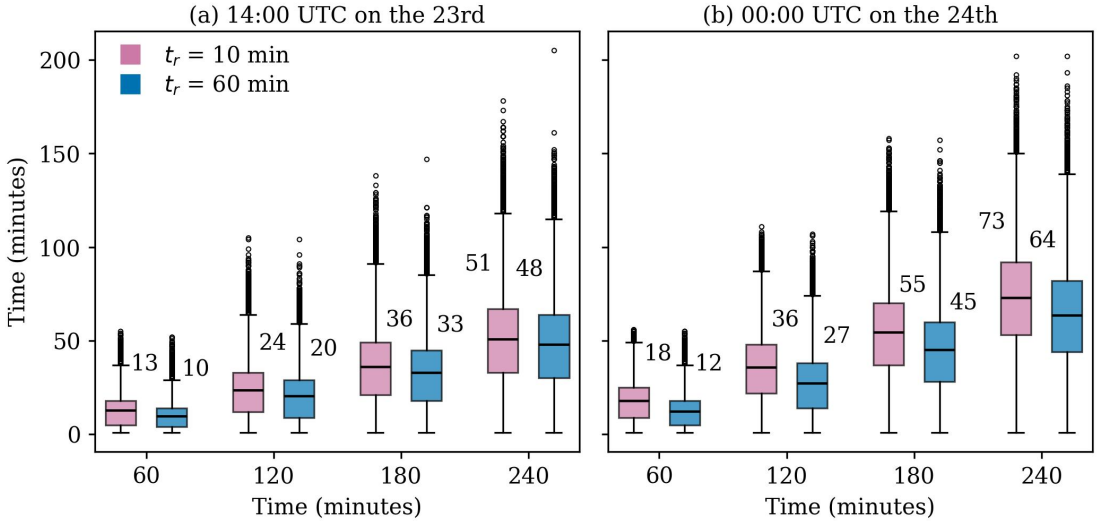
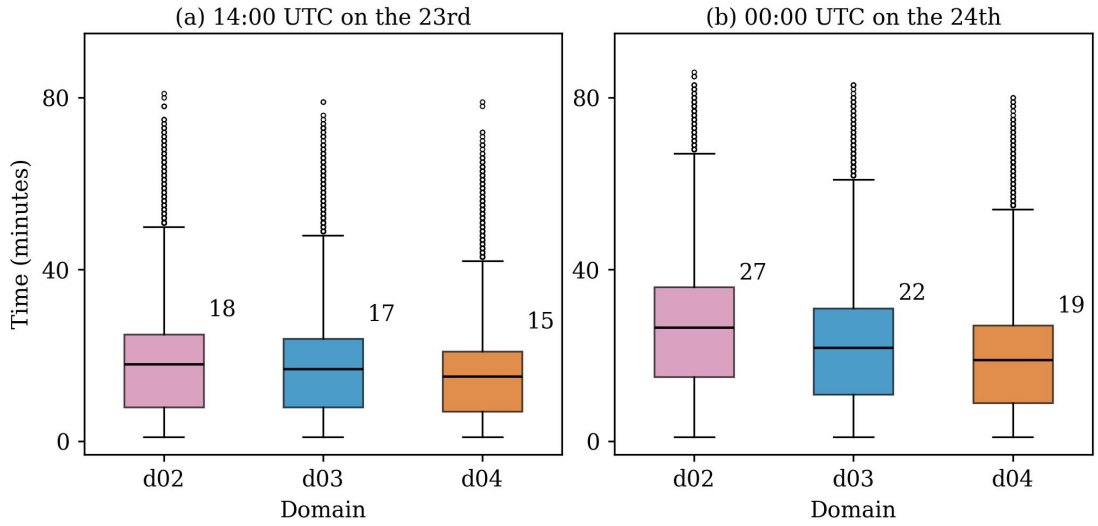


Fig. 10:



- *Caption Table 1 not on same page*

In the revised manuscript, the original Table 1 has been renumbered as Table 3. We have adjusted the layout so that its caption is now presented on the same page as the table for better readability. In addition, we have added the results for the $t_r = 60$ min release experiments (Lines 469-474).

Table 3. Parcel transport statistics for t_r = 10 min and 60 min releases across simulation domains and release times, focusing on the first 90 or 120 min. Statistics include the peak instantaneous arrival rate, peak arrival time, and cumulative arrival rate at the end of the analysis period. For 90-min analyses, all domains are cropped to d04; for 120-min analyses, d02 and d03 are cropped to d03.

Domain	Release timing (UTC)	Analysis period (min)	Peak (%)	Peak time (min)	Final cumulative (%)	Peak (%)	Peak time (min)	Final cumulative (%)	Cropped to
			t_r = 10 min			t_r = 60 min			
d02	23 14:00	90	2.82	14	89.38	1.50	61	80.80	d04
	23 22:00	90	2.84	14	90.64	1.61	61	84.97	d04
	24 00:00	90	3.60	14	96.02	1.56	60	85.59	d04
	24 02:00	90	3.41	14	95.44	1.57	53	85.26	d04
	24 06:00	90	3.31	14	92.04	1.56	59	85.10	d04
d03	23 14:00	90	2.47	15	86.35	1.31	55	73.89	d04
	23 22:00	90	2.16	16	82.72	1.45	66	75.44	d04
	24 00:00	90	2.50	16	89.18	1.42	65	77.16	d04
	24 02:00	90	2.49	15	87.14	1.35	66	73.67	d04
	24 06:00	90	2.30	17	85.64	1.38	64	76.19	d04
d04	23 14:00	90	2.02	18	80.14	1.24	64	67.07	d04
	23 22:00	90	1.86	18	76.86	1.28	66	67.51	d04
	24 00:00	90	2.04	16	83.35	1.26	63	69.77	d04
	24 02:00	90	1.98	18	80.04	1.16	66	63.94	d04
	24 06:00	90	1.82	17	77.59	1.29	65	66.77	d04
d02	23 14:00	120	2.82	14	94.88	1.50	61	91.78	d03
	23 22:00	120	2.84	14	95.50	1.61	61	94.79	d03
	24 00:00	120	3.60	14	98.72	1.56	60	95.29	d03
	24 02:00	120	3.41	14	98.44	1.57	53	95.06	d03
	24 06:00	120	3.31	14	96.08	1.56	59	94.63	d03
d03	23 14:00	120	2.47	15	92.63	1.31	55	87.43	d03
	23 22:00	120	2.16	16	90.78	1.45	66	89.01	d03
	24 00:00	120	2.50	16	95.17	1.42	65	90.57	d03
	24 02:00	120	2.49	15	93.76	1.35	66	87.13	d03
	24 06:00	120	2.30	17	93.58	1.38	64	89.79	d03

Reference

Wood, R.: Assessing the potential efficacy of marine cloud brightening for cooling Earth using a simple heuristic model, Atmos. Chem. Phys., 21, 14507–14533, https://doi.org/10.5194/acp-21-14507-2021, 2021.